Int. J. Electrochem. Sci., 15 **(2020)** 7163 – 7174, doi: 10.20964/2020.08.67

International Journal of
ELECTROCHEMICAL
SCIENCE
www.electrochemsci.org

Rapid Fabrication of of $Li_7La_3Zr_2O_{12}$ Solid Electrolyte with Enhanced Lithium Ionic Conductivity by Microwave Sintering

Yanhua Zhang[1,2,*], *Wenjia Luo*[1], *Dongwei Hu*[1], *Yuxin Deng*[1], *Yuan Chen*[1,*], *Jiadong Deng*[3]

[1] Hubei Provincial Key Laboratory of Green Materials for Light Industry, Hubei University of Technology, Wuhan, 430068, China
[2] Collaborative Innovation Center of Green Light-weight Materials and Processing, Hubei University of Technology, Wuhan, 430068, China
[3] School of Automotive Engineering, Wuhan University of Technology, Wuhan 430070, China
[*]E-mail: yanhzhang@139.com, chen.yuan@hbut.edu.cn

Received: 3 March 2020 / *Accepted:* 11 May 2020 / *Published:* 10 July 2020

Traditional preparation method of solid electrolyte $Li_7La_3Zr_2O_{12}$ requires a very long sintering holding time (> 36 hours). A efficient and mass production method, microwave sintering, is utilized to prepared LLZO by which the sintering time is reduced to be 2 ~ 4 h. Results show that cubic phase LLZO can be obtained at 1150 °C ~ 1200 °C. With the increase of holding time from 1 h to 4 h, tetragonal LLZO transforms to cubic which suggests extra thermal energy is generated by coupling dielectric loss with microwave. Pellet sintered with 4 h reaches the highest ionic conductivity of 3.1×10^{-4} S cm^{-1}. Long holding time of 6 h will take away a lot of Li from the grain to form excess glass-like phase which is not favorable for conductivity.

Keywords: Solid electrolytes; $Li_7La_3Zr_2O_{12}$; Microwave sintering; Li^+ ionic conductivity

1. INTRODUCTION

Commercial lithium ion batteries often use organic electrolytes which has a Li^+ ionic conductivity of up to ~10^{-2} S cm^{-1}. This provides favorable conditions for achieving high rate performance of the lithium ion batteries. However, organic electrolytes are prone to leakage and have the risk of burning and explosion. In order to fundamentally eliminate the safety hazards of organic electrolytes, solid electrolytes emerge as the times require which have received wide attention [1-4]. All-solid-state lithium battery based on solid electrolyte can use lithium metal (3860 mAh g^{-1}) as the negative electrode which could achieve high energy density. Comparing with organic electrolytes, the solid electrolytes is expected to eliminates the generation of lithium dendrites and also prevents the metal lithium anode from forming an unstable SEI film which result in capacity attenuation and coulombic efficiency degradation [5-8]. Therefore, the strategy of assembling lithium metal batteries using solid electrolytes is expected to completely solve the safety hazards of lithium metal batteries, while meeting the energy demand of new energy vehicles for chemical power sources. Among various types of solid electrolyte candidates, garnet type $Li_7La_3Zr_2O_{12}$ (LLZO) has attracted great attention due to its high room temperature Li^+ ionic conductivity (10^{-3} ~ 10^{-4} S cm^{-1}), wide electrochemical window ($\geq$ 5 V) which could match high voltage electrodes, and relatively stability in air which make the procedure of preparation and processing facile [9-12]. In order to realize the application of LLZO in all-solid-state lithium battery, the low cost, high efficiency preparation method as well as achieving high Li^+ ionic conductivity is critical.

The most common preparation method at present is the traditional solid state reaction method. It typically requires at least 36 hours of holding time in the preparation of LLZO solid electrolytes and needs intermittent grinding and repeated heat treatment, which makes this method very inefficient [13-15]. Moreover, the long sintering time often result in impurity phases due to lithium loss at high temperature. Such as, Song et al. [13] prepared Gd^{3+}-doped LLZO by traditional solid state reaction method at sintering temperature of 1220 °C with holding time as long as 36 hours, not counting the pre-sintering time at 950 °C for 12 h. The optimized Li^+ ionic conductivity is about 2.3×10^{-4} S cm^{-1} with 0.2 Gd^{3+} doping content of $Li_{7.2}La_3Zr_{1.8}Gd_{0.2}O_{12}$. For solid electrolytes, higher density generally leads to higher Li^+ ionic conductivity. Most researchers prefer high-pressure technology, such as cold isostatic pressing (CIP) in which LLZO green body is pressed at high pressure or hot isostatic pressing (HIP) in which LLZO green body are pressed during sintering process, to gain high density of LLZO [16, 17]. For example, Qin et al. [16] apply the HIP treatment at 120 MPa and 1160 °C under an Ar atmosphere to prepared LLZO. It is found that the HIP-treated Ga-doped LLZO shows a dense relative density of 97.5% and two times higher Li^+ ionic conductivity of the untreated one. However, such synthesis process is complex which needs high pressure, high vacuum and protective atmosphere such as Ar and generally only one pellet can be sintered at a time which makes it difficult to carry out mass production and commercial application.

Microwave sintering technology is a new process for preparing materials by using a special wavelength band of a microwave which is very different from the traditional solid state reaction method. In traditional sintering method, heat is conducted from outside to inside of the sample which result in long sintering time and large energy consumption, while in the microwave sintering technology, heat is generated inside the sample by coupling the dielectric loss of the material with the microwave electromagnetic field to reach the sintering temperature [18-20]. There is no need for heat conduction during microwave heating, that is, it is instantaneous without thermal inertia, which means that the heat source can be cut off instantaneously and heat up in time, reflecting the characteristics of energy saving and precise control. The special way of heat conduction and the rapid heating rate (up to 1000 °C min^{-1}) are highly expected to reduce the manufacturing cost and improve the preparation efficiency. Besides, the rapid heating rate can suppress the growth of the grain structure, obtain the ultrafine grain structure material, and significantly improve the microstructure of the material. So far, plenty of ceramic materials such as Al_2O_3, B_4C, Y_2O_3-ZrO_2, SiO_2, TiO_2 and ZnO have been successfully prepared by microwave sintering technology and small batch industrialization by applying this technology has been achieved [18-21].

In this work, microwave sintering technology is applied to prepare LLZO which aimed at significantly shortening the sintering holding time and lower the sintering temperature. The effect of sintering temperature and holding time on the phase compositions, microstructure and Li^+ ionic conductivity of the sintered samples is comprehensively investigated. And the effect of alumina and magnesia crucible on the microstructure and properties of LLZO were also studied.

2. EXPERIMENTAL PROCEDURES

The experimental material were high-purity Li_2CO_3 (purity 99.9 %, produced by Aladdin), La_2O_3 (purity 99.9 %, produced by Sinopharm Chemical Reagent Co., Ltd., China), ZrO_2 (purity 99.9 %, produced by Oriental Zirconium Industry). The reaction materials were weighed according to the molar ratio of Li, La, and Zr elements of 7 : 3 : 2. 1.5 wt% γ-Al_2O_3（99 %，produced by Maclin） was added as additive. Excess of 10% lithium source was added to compensate for the loss of lithium at high temperatures.

Firstly, the powders were mixed by ball-milled with isopropyl alcohol for 6 h. And then the powders were dried in vacuum oven to remove the isopropyl alcohol. Secondly, the mixed powders were calcined at 950 °C for 6 h in an electric furnace and then pressed into a pellet of 18 mm in diameter under 120 MPa. Subsequently, the pellets were sintered by microwave sintering system (Mobile Lab Workstation) with a microwave frequency of 2.45 GHz and a power of 4 kW. Sintering process was performed at the temperature range of 1000 °C to 1230 °C with the holding time of 1 h to 6 h by microwave sintering. The subsequent heating rate was set as 200 °C min^{-1} under 600 °C, 50 °C min^{-1} under 900 °C and lowered to 1 ~ 2 °C min^{-1} near the target temperature. Alumina and magnesia crucibles were separately used to sintering the samples.

The phase structure of the LLZO samples were characterized by X-ray diffraction (XRD, Rigaku Ultima III) with Cu Kα radiation over the range of 10 ~ 70 ° (2θ). The microstructure of the LLZO pellets was observed by field-emission scanning electron microscopy (FESEM, FEI-Quanta-250). The Li^+ ionic conductivity was measured using an electrochemistry impedance spectrometer (ZAHNER Xpot. Germany) in the frequency range from 10 Hz to 4 MHz at elevated temperature range of 20 ~ 140 °C with 10 mV perturbation amplitude. Pt was sputtered on both sides of the pellet as ionic blocking electrodes. Impedances were determined from the intercepts of the relevant capacitive arcs at the real axes in the Nyquist plots and conductivities were calculated using the following equation:

$$\sigma = (1/Z)(L/A) \qquad (1)$$

where σ is the ionic conductivity, Z is the impedance, L is the pellet thickness, and A is the pellet area. Typical dimensions of the pellets were about 2.0 ~ 2.2 mm in thickness, 16 mm in diameter.

3. RESULTS AND DISCUSSION

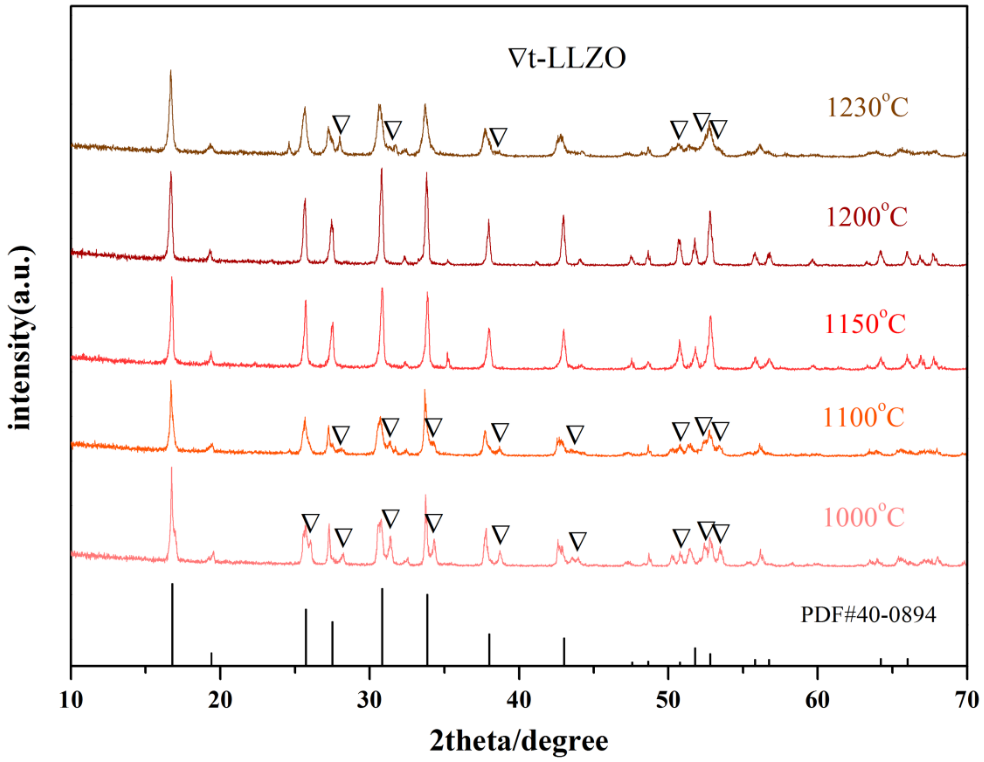

Figure 1. XRD spectra of LLZO samples sintered by microwave at temperatures from 1000 °C to 1230 °C (▽characteristic peaks of the tetragonal LLZO phase. PDF#40-0894 is a reference for cubic garnet).

Fig. 1 shows the XRD patterns of samples sintered by microwave technology at temperatures of 1000 ~ 1230°C for 4 hours. At low sintering temperature of 1000 °C, LLZO is a tetragonal phase for each diffraction peak splits to two peaks. With the temperature increase to 1100 °C, the two splitting peaks are merging into one peak leaving the main peaks of cubic phase LLZO with little shoulders, which suggests a mixture of cubic and tetragonal phases [22]. With further increase of the temperature to 1150 °C ~ 1200 °C, all the shoulders disappears, each peak is single and sharp which indexed to pure cubic phase LLZO. It is noted that phase transition from tetragonal to cubic occurs at about 1100 °C ~ 1150 °C. However, at higher temperature of 1200 °C, the cubic phase LLZO transforms into tetragonal phase again. This indicates that cubic phase can only exist stably in a narrow temperature range of 1150 °C ~ 1200 °C.

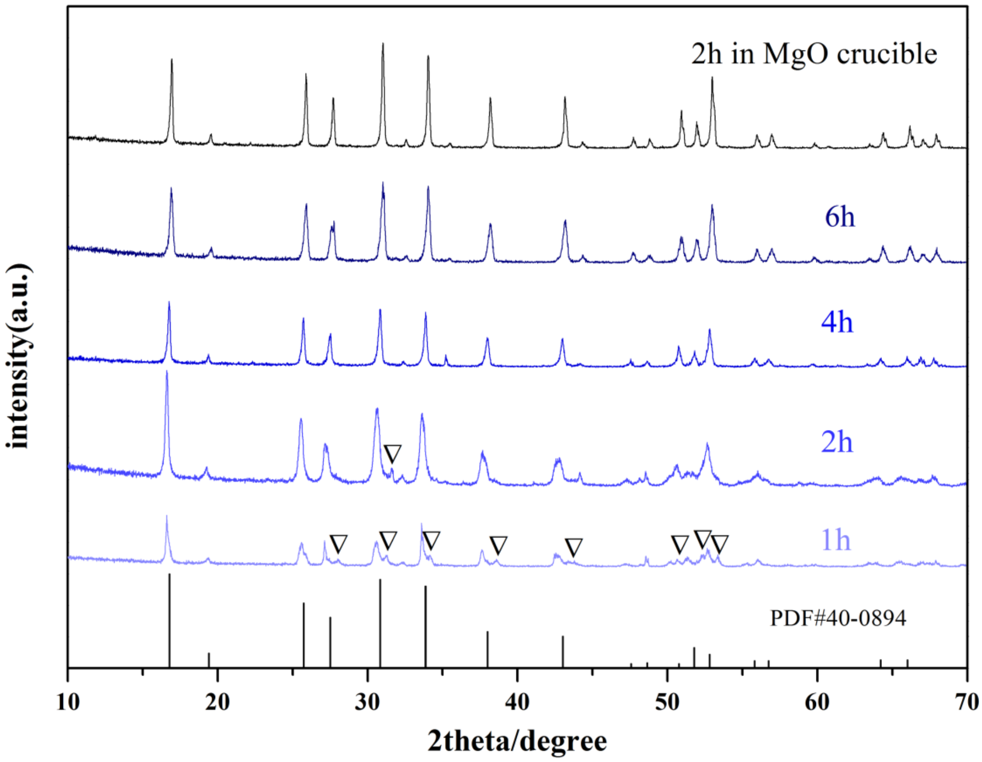

Figure 2. XRD spectra of LLZO samples sintered by microwave sintering with holding time from 1 h to 6 h at 1150 ºC. (▽characteristic peaks of the tetragonal LLZO phase. PDF#40-0894 is a reference for cubic garnet).

Fig. 2 shows the XRD pattern of microwave sintering with various holding time at 1150 ºC. As can be seen from Fig. 2, with short holding time of 1 h, each diffraction peak splits into two peaks which indicate tetragonal phase of LLZO. With the holding time increased to 2 h, most of the splitting peaks merge into one broad peak which indexed to a mixture of tetragonal and cubic phases. With the holding time further increased to 4 h ~ 6 h, all of the diffraction peaks are narrow and sharp without any characteristic peaks of tetragonal phase, suggesting pure cubic phase of LLZO is obtained. This indicates that, with the increase of the holding time from 1 h to 4 h, LLZO undergo a phase transition from tetragonal to cubic phase. Anyway, it is well-known that phase transition is athermal. The driving force of phase transition is temperature, that is, the phase transition degree only changes with temperature not changes with the holding time. The LLZO phase transition suggests that extra thermal is generated with the increase of the holding time from 1 h to 4 h during microwave sintering. It has been reported that ceramics such as ZrO_2 and Al_2O_3 et al. generate thermal due to polarization phenomenon under microwave electromagnetic field [18, 20]. This extra thermal might be produced by LLZO absorbing microwave energy and converts it into thermal energy under microwave electromagnetic field.

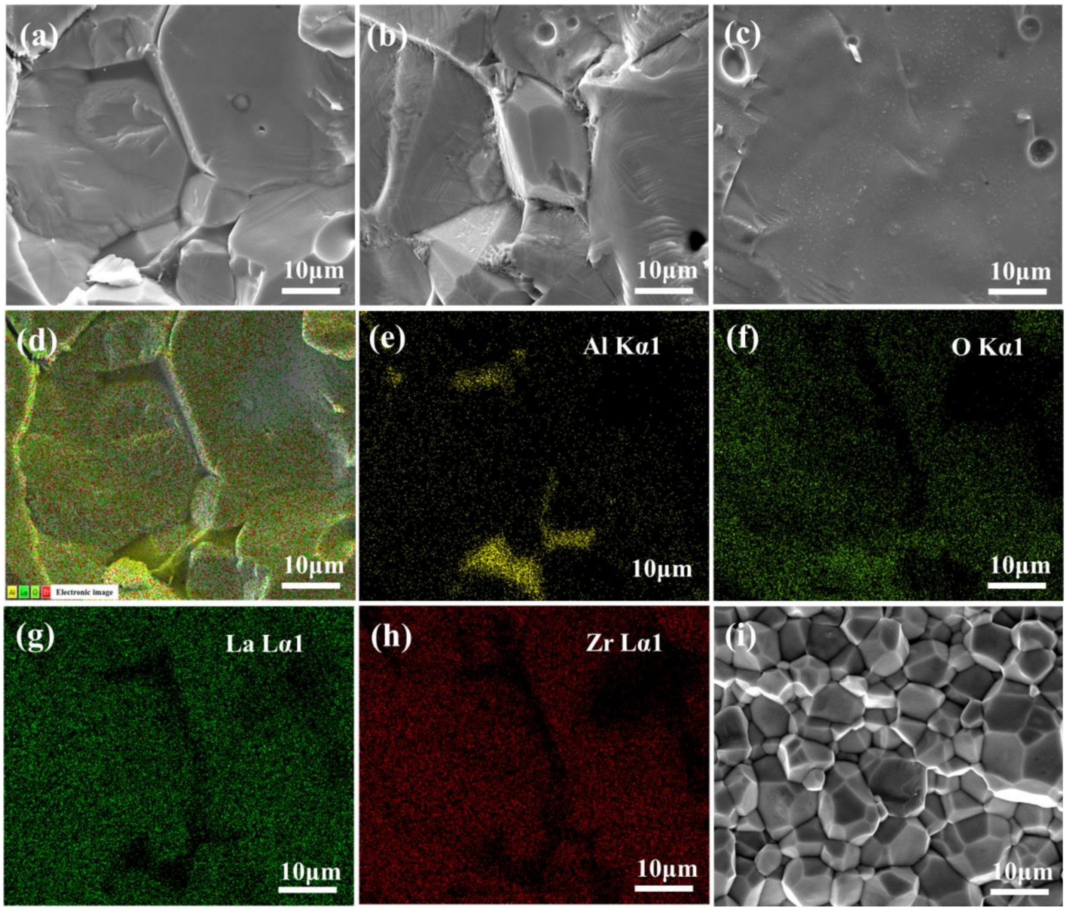

Figure 3. SEM micrographs of the cross-sections of the LLZO samples sintered by microwave with various holding time (a) 2 h (b) 4 h (c) 6 h in Al_2O_3 crucibles, (d) ~ (h) EDS area distribution of elements of Al， O， La, and Zr of (a), and (i) 2 h in MgO crucibles.

Fig. 3 (a) ~ (c) shows the SEM micrographs of the cross-sections of the LLZO samples sintered by microwave with various holding time (a) 2 h (b) 4 h (c) 6 h in Al_2O_3 crucibles. For the pellet sintered with 2 h in Al_2O_3 crucibles (Fig. 3 (a)), the particles contact tightly with each other and the fracture is almost transgranular. A glass-like phase is clearly observed at the grain boundary in the sample sintered for 2 h. With the increase of the holding time from 2 h to 6 h, the content of glass-like phase seems to have become more, no crystal particles are visible and some open pores can be observed in the pellet sintered for 6 h. This indicates that long sintering time will cause excessive pore number and size. Fig. 3 (d) ~ (h) shows the EDS area distribution of elements of Al, O, La, and Zr of sample sintered for 2 h. As can be clearly seen, Al and O elements are densely distributed at the grain boundary without La and Zr elements. This suggests that the glass-like phase most probably is a Li-Al-O amorphous phase which is consistent with the report of Huang et al. [23]. The increase of the glass-like phase with the holding time suggest that the content of Al^{3+} contaminated from the Al_2O_3 crucibles increase with the increase of the holding time. As a comparison, the sample is sintered by MgO crucibles at the same experimental condition for 2 h. As can be seen from Fig. 3 (I), the grain boundary is very clean, none of visible glass-like phase can be observed.

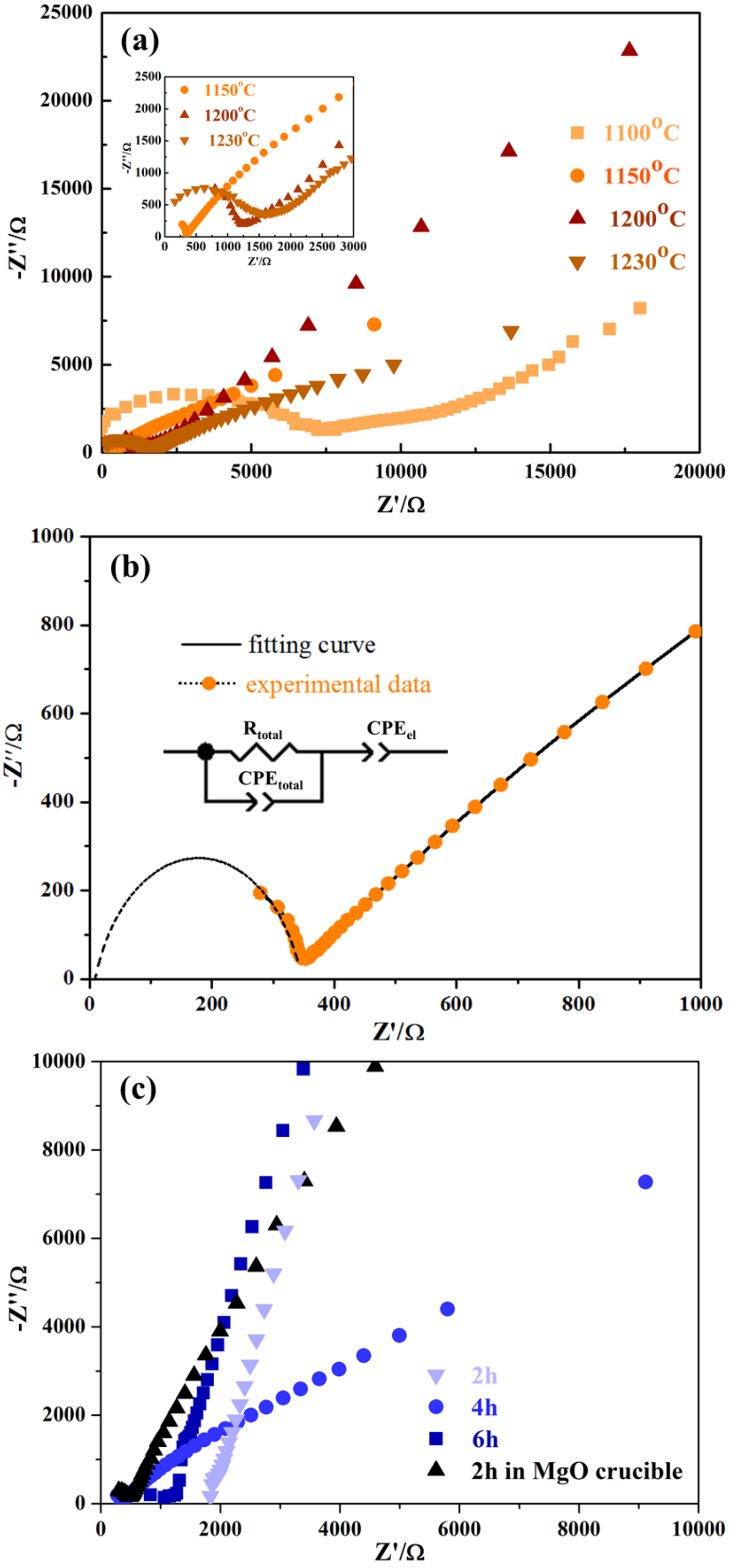

Figure 4. (a) Nyquist plots of the samples sintered by microwave with various temperature 1100 °C ~ 1230 °C measured at room temperature, (b) equivalent circuit of ($R_{total}CPE_{total}$)CPE_{el} fitting curve of the experimental data of the pellet sintered at 1150 °C, (c) Nyquist plots of the samples sintered with various holding time of 2 ~ 6 h in Al_2O_3 crucibles and 2 h in MgO crucibles at 1150 °C.

The room temperature impedance spectrum of the sintered samples with various temperature of 1100 °C ~ 1230 °C and holding time of 2 ~ 6 h is shown in Fig. 4 (a) and (c). All curves contain a deformed semicircle at high frequency and a tail at low frequency, which correspond to the total resistance of LLZO and the ionic blocking electrode, respectively. An equivalent circuit of $(R_{total}CPE_{total})CPE_{el}$ is used to analyze the data where R is total resistances and CPE is constant phase elements [14], as shown in Fig. 4 (b). The total ionic conductivity is calculated by using the semicircle intercept on the Z' axis at high frequency and the sample dimensions.

Table 1 summarizes 25 °C Li^+ conductivity of LLZO samples sintered at various temperatures and holding time in Al_2O_3 crucible and 2 h in MgO crucible. As shown in Table 1, the pellets sintered at 1150 °C and 1200 °C have higher Li^+ ionic conductivity of 3.1×10^{-4} S cm^{-1} and 1.1×10^{-4} S cm^{-1}, compared with that of 1100 °C and 1230 °C. It is well-known that the Li^+ ionic conductivity of tetragonal phase is two orders of magnitude lower than that of the cubic phase. The higher conductivity of pellets sintered at 1150 °C and 1200 °C is mainly due to the high purity of cubic phase of LLZO while it is a mixture phase of cubic and tetragonal at 1100 °C and 1230 °C as discussed in the XRD results. The slight higher Li^+ ionic conductivity of the pellet sintered at 1150 °C (3.1×10^{-4} S cm^{-1}) than that of 1200 °C (1.1×10^{-4} S cm^{-1}) probably due to the different Li^+ concentration in the grain of LLZO according to the study of zhang et al. [24]. The higher sintering temperature at 1200 °C will result in excess loss of Li which might slightly decrease the conductivity.

In addition to sintering temperature, the holding time of microwave sintering has a significant effect on the Li^+ ionic conductivity. As show in Fig. 4 (c) and Table 1, with shorter holding time of 2 h, the Li^+ ionic conductivity is low of 0.55×10^{-4} S cm^{-1}. This is because with shorter sintering time (2 h), LLZO index to a mixture of tetragonal and cubic phases. Pellet sintered with 4 h holding time reaches the highest ionic conductivity of 3.1×10^{-4} S cm^{-1} compared with that of 6 h (0.83×10^{-4} S cm^{-1}) and 2 h (0.55×10^{-4} S cm^{-1}). It is concluded that, with short holding time of 2 h, the incomplete of phase transition from tetragonal to cubic is the main reason for the low Li^+ ionic conductivity, while long holding time of 6 h also results in the decrease of conductivity. The decrease of Li^+ ionic conductivity with long holding time (6 h) might be related to the Li loss during sintering and the excess glass-like phase formed at the grain boundary. It is noted that the total ionic conductivity consists of the grain conductivity and the grain boundary conductivity and the total conductivity is mainly determined by the grain conductivity [24]. Generally, the glass-like phase is favorable for improving the Li^+ grain boundary conductivity, however, the excess formation of glass-like phase will take away a lot of Li from the grain which decrease the grain conductivity [23]. Therefore, excess formation of glass-like phase with 6 h holding time is not favorable for improving the total Li^+ ionic conductivity. Besides, the Li^+ ionic conductivity for the pellet sintered for 2 h in MgO crucible (1.8×10^{-4} S cm^{-1}) is much higher than that of 2 h in Al_2O_3 crucible (0.55×10^{-4} S cm^{-1}) and very close to that of pellet sintered in Al_2O_3 for 4 h (3.1×10^{-4} S cm^{-1}). This is mainly due to LLZO is cubic phase in MgO for 2 h while it is a mixture of cubic and tetragonal phase in Al_2O_3 for 2 h. This indicates that pellets sintered in MgO crucible is in favor of phase transition from tetragonal to cubic phase.

Table 1. 25 °C Li^+ conductivity of LLZO samples sintered at various temperatures and holding time in Al_2O_3 crucible and 2 h in MgO crucible.

	1100 °C	1150 °C	1200 °C	1230 °C
2 h	n/a	0.55×10^{-4}	n/a	n/a
4 h	1.3×10^{-5}	3.1×10^{-4}	1.1×10^{-4}	0.66×10^{-4}
6 h	n/a	0.83×10^{-4}	n/a	n/a
2 h in MgO crucible	n/a	1.8×10^{-4}	n/a	n/a

Fig. 5 (a) shows the Nyquist plot of the impedance spectrum measured at temperatures between 20 °C and 140 °C for the cubic phase LLZO prepared by microwave sintering at 1150 °C for 4 h. The temperature dependence of the total ionic conductivity (Arrhenius plot) is shown in Fig. 5 (b). It can be expressed using the Arrhenius equation:

$$\sigma = \frac{A}{T} exp\ (\frac{-E_a}{k_B T}) \qquad (2)$$

where σ (S cm^{-1}) is the ionic conductivity, T (K) is the absolute temperature, A is the pre-exponential constant, R is the Boltzmann constant and Ea (eV) is the activation energy for the Li^+ ionic conductivity. According to the Arrhenius equation, the total conduction activation energy is determined by the slope of the log (σ T) and 1/T plots. The low activation energy indicates the low barrier for Li^+ transportation to overcome. The activation energy of the total Li^+ ionic conductivity of the LLZO in the temperature range of 20 ~ 140 °C is calculated to be 0.32 eV which is exactly close to the reported LLZO solid electrolytes prepared by solid state reaction method (0.31 eV) [25].

Above all, the cubic phase LLZO prepared by microwave sintering technology has total ionic conductivity (3.1×10^{-4} S cm^{-1}) as high as that of the traditional solid state reaction method (3.0×10^{-4} S cm^{-1}). However, microwave sintering technology has an extremely short sintering time of 2 ~ 4 h and relative lower sintering temperature of 1150 °C compared to 36 h and 1230 °C of the traditional solid state reaction method. The significance reduction of sintering time and lower sintering temperature is mainly because that the heat is generated inside the sample by coupling the dielectric loss of the LLZO ceramics with the microwave electromagnetic field, thus achieving densification. Besides, such synthesis process can produce large quantities of pellets in batches which make mass production and commercial application possible. The above advantages indicate that microwave sintering technology is a particularly efficient method for preparing high Li^+ ionic conductivity cubic phase LLZO solid electrolytes.

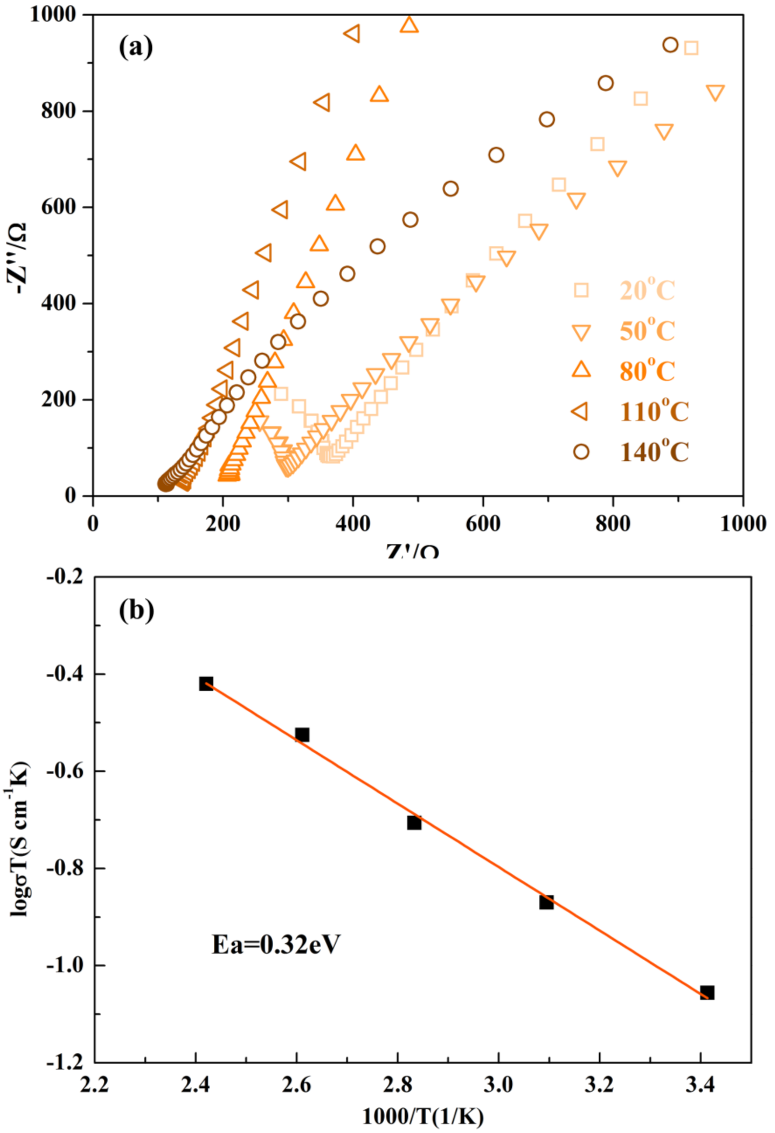

Figure 5. (a) Nyquist plots (frequency range: 10 Hz ~ 4 MHz) and (b) Arrhenius plot for the total (bulk + grain boundary) ionic conductivity measured at temperatures between 20 °C and 140 °C of LLZO samples prepared by microwave sintering at 1150 °C for 4 h.

Table 2 shows the comparison of properties and process conditions of cubic phase LLZO prepared by microwave sintering and other methods. The traditional solid-state reaction method is often used which has the disadvantage of too long sintering time of 12 ~ 36 h. The LLZO precursor prepared by solution method has a smaller particle size, which is beneficial to reduce the sintering time (6 h). However, the density is usually not too high due to plenty of voids left by the decomposition of organics during the sintering process which result in relatively low Li^+ conductivity of 2×10^{-4} S cm^{-1}. While for the microwave sintering method, it has short sintering time of less than 4 h and relatively low sintering temperature of 1150 °C as well as possessing relatively high Li^+ conductivity of 3.1×10^{-4} S cm^{-1}. The short sintering time and low sintering temperature indicates that the microwave sintering technology is effectively method for preparing high performance LLZO.

Table 2. Comparison of cubic LLZO ceramics fabricated by several methods.

Methods	Manufacturing conditions	Total ionic conductivity/S cm^{-1}
Solid-state reaction [26] [27] [28]	1125 ºC – 12h [28]	2.56×10^{-4}
Solution based methods [29] [30] [31]	1200 ºC – 6h [31]	2×10^{-4}
This work	1150 ºC – 4h	3.1×10^{-4}

4. CONCLUSION

High performance cubic phase $Li_7La_3Zr_2O_{12}$ solid electrolyte was successfully prepared by microwave sintering technology. The effect of sintering temperature and holding time on the microstructure and Li^+ ionic conductivity was studied.

(1)Pure cubic phase LLZO can be obtained at 1150 ºC ~ 1200 ºC, too high or too low temperature will result in the generation of tetragonal phase. With the increase of the holding time from 1 h to 4 h, LLZO undergo a phase transition from tetragonal to cubic phase which suggests that extra thermal energy is generated by LLZO absorbing microwave energy under microwave electromagnetic field.

(2) Pellet sintered with 4 h holding time at 1150 ºC reaches the highest ionic conductivity of 3.1×10^{-4} S cm^{-1} and low activation energy of 0.32 eV. Long holding time of 6 h will take away a lot of Li from the grain to form excess glass-like phase which is not favorable for the enhancement of total ionic conductivity. The Li^+ ionic conductivity of pellet sintered in MgO crucible for 2 h (1.8×10^{-4} S cm^{-1}) is much higher than that in Al_2O_3 crucible (5.5×10^{-5} S cm^{-1}) which is mainly due to the complete phase transition.

(3) Compare with the traditional solid state reaction method, the benefits of extremely short sintering time of 2 ~ 4 h, relatively lower sintering temperature and mass production indicate that microwave sintering technology is a particularly efficient method for preparing high performance LLZO solid electrolytes.

ACKNOWLEDGEMENT
This work is financially supported by the National Natural Science Foundation of China (No. 51902096 and No. 51805391), the Natural Science Fund of Hubei Province (No. 2019CFB304) and the State Key Laboratory of Advanced Technology for Materials Synthesis and Processing (Wuhan University of Technology, No. 2019-KF-14).

References

1. Z.P. Wan, D.N. Lei, W. Yang, C. Liu, K. Shi, X.G. Hao, L. Shen, W. Wei, B.H. Li, Q.H. Yang, F.Y. Kang and Y.B. He*, Adv. Funct. Mater.,* 29 (2019) 1805301.
2. R. Pfenninger, M. Struzik, I. Garbayo, E. Stilp and J.L.M. Rupp, *Nat. Energy,* 4 (2019) 475.

3. X. Li, R.X. Li, S.Y. Chu, K.M. Liao, R. Cai, W. Zhou and Z.P. Shao, *J. Alloys Compd.,* 794 (2019) 347.
4. D. Rettenwander, *Chem-US,* 5 (2019) 1695.
5. W.D. Richards, L.J. Miara, Y. Wang, J.C. Kim and G. Ceder, *Chem. Mater.,* 28 (2015) 266.
6. C.L. Tsai, V. Roddatis, C.V. Chandran, Q.L. Ma, S. Uhlenbruck, M. Bram, P. Heitjans and O. Guillon, *ACS Appl. Mater. Interfaces,* 8 (2016) 10617.
7. F.A.G. Daza, M.R. Bonilla, A. Llordes, J. Carrasco and E. Akhmatskaya, *ACS Appl. Mater. Interfaces,* 11 (2018) 753.
8. J.C. Bachman, S. Muy, A. Grimaud, H.H. Chang, N. Pour, S.F. Lux, O. Paschos, F. Maglia, S. Lupart, P. Lamp, L. Giordano and Y. Shao-Horn, *Chem. Rev.,* 116 (2015) 140.
9. G. Vardar, W.J. Bowman, Q.Y. Lu, J.Y. Wang, R.J. Chater, A. Aguadero, R. Seibert, J. Terry, A. Hunt, I. Waluyo, D.D. Fong, A. Jarry, E.J. Crumlin, S.L. Hellstrom, Y.M. Chiang and B. Yildiz, *Chem. Mater.,* 30 (2018) 6259.
10. P. Canepa, J.A. Dawson, G.S. Gautam, J.M. Statham, S.C. Parker and M.S. Islam, *Chem. Mater.,* 30 (2018) 3019.
11. H. Koshikawa, S. Matsuda, K. Kamiya, M. Miyayama, Y. Kubo, K. Uosaki, K. Hashimoto and S. Nakanishi, *J. Electroanal. Chem.,* 835 (2019) 143.
12. N.J. Taylor, S. Stangeland-Molo, C.G. Haslam, A. Sharafi, T. Thompson, M. Wang, R. Garcia-Mendez and J. Sakamoto, *J. Power Sources,* 396 (2018) 314.
13. S.D. Song, B.T. Chen, Y.L. Ruan, J. Sun, L.M. Yu, Y. Wang and J. Thokchom, *Electrochim. Acta,* 270 (2018) 501.
14. S. Ohta, T. Kobayashi and T. Asaoka, *J. Power Sources,* 196 (2011) 3342.
15. M. Kotobuki, K. Kanamura, Y. Sato and T. Yoshida, *J. Power Sources,* 196 (2011) 7750.
16. S.Y. Qin, X.H. Zhu, Y. Jiang, M.E. Ling, Z.W. Hu and J.L. Zhu, *Funct. Mater. Lett.,* 11 (2018) 1850029.
17. I.N. David, T. Thompson, J. Wolfenstine, J.L. Allen and J. Sakamoto, *J. Am. Ceram. Soc.,* 98 (2015) 1209.
18. Y. Cheng, S. Sun and H. Hu, *Ceram. Int.,* 40 (2014) 16761.
19. S.G. Huang, L. Li, O.V.D. Biest and J. Vleugels, *J. Eur. Ceram. Soc.,* 27 (2007) 689
20. E. Savary, S. Marinel, F. Gascoin, Y. Kinemuchi, J. Pansiot and R. Retoux, *J. Alloys Compd.,* 509 (2011) 6163.
21. E. Ghasai, A. Pakseresht, F. Safari-kooshali, M. Agheli and T. Ebadzadeh, *J. Mater. Res. Technol.,* 4 (2015) 411.
22. Y.H. Zhang, F. Chen, R. Tu, Q. Shen and L.M. Zhang, *J. Power Sources,* 268 (2014) 960.
23. X. Huang, Y. Lu, H.J. Guo, Z. Song, T.P. Xiu, M.E. Badding and Z.Y. Wen, *ACS Appl. Energy Mater.,* 1 (2018) 5355.
24. Y.H. Zhang, F. Chen, R. Tu, Q. Shen, X.L. Zhang and L.M. Zhang, *Solid State Ionics,* 284 (2016) 53.
25. R. Murugan, V. Thangadurai and W. Weppner, *Angew. Chem. Int. Ed.,* 46 (2007) 7778.
26. Z.L. Hu, H.D. Dong, H.B. Ruan, R. Hu, Y.Y. Su and L. Zhang, *Ceram. Int.,* 42 (2016) 12156.
27. M. Kotobuki, K. Kanamuraa, Y. Sato and T. Yoshida, *J. Power Sources,* 196 (2011) 7750.
28. B.G. Yan, M. Kotobuki and J.C. Liu, *Mater. Technol.,* 31 (2016) 623.
29. J. Wolfenstinea, E. Rangasamy, J.L.Allena and J. Sakamoto, *J. Power Sources,* 208 (2012) 193.
30. K. Chen, M. Huang, Y. Shen, Y.H. Lin and C.W.Nan, *Electrochim. Acta,* 80 (2012) 133.
31. E.A. Il'ina, O.L. Andreev, B.D. Antonov and N.N. Batalov, *J. Power Sources,* 201 (2012) 169.